ELSEVIER

Sensors and Actuators B 57 (1999) 17–27

SENSORS AND ACTUATORS B CHEMICAL

www.elsevier.nl/locate/sensorb

Effect of micro-electrode geometry on response of thin-film poly(pyrrole) and poly(aniline) chemoresistive sensors

Paul Ingleby [a,*], Julian W. Gardner [a], Philip N. Bartlett [b]

[a] *Division of Electrical and Electronic Engineering, School of Engineering, University of Warwick, Coventry, CV4 7AL, UK*
[b] *Department of Chemistry, University of Southampton, Southampton, SO17 1BJ, UK*

Received 14 September 1998; received in revised form 16 December 1998; accepted 13 January 1999

Abstract

The response of four different electrochemically prepared resistive conducting polymer sensors to ethanol vapour has been investigated. A theoretical model is developed relating the effect of the micro-electrode geometry on both the steady-state and transient responses. Our theory is compared with experimental results gathered when exposing the sensors to different concentrations of ethanol vapour in air at different relative humidities. The information gained from this comparison is finally used to determine the nature of the polymers using the diffusionbreaction case diagram originally proposed by Gardner et al. [J.W. Gardner, P.N. Bartlett, K. Pratt, Modelling of gas-sensitive conducting polymer devices, IEE Proc.: Circuits, Devices and Systems 142 (1995) 321-333].

Keywords: Polymer sensor; Ethanol; Diffusion reaction

1. Introduction

A planar chemoresistive sensor generally consists of a pair of inert, coplanar electrodes coated onto an insulating substrate across which a vapour-sensitive film has been deposited. Changes in the electrical conductance of the film can then be monitored while the sensor is exposed to a test vapour [1]. The characteristics of this device usually depend upon the choice of polymer and vapour, electrode geometry and ambient humidity. In this paper we report on the effect of the electrode geometry on the response of conducting polymer resistive gas sensors. The work is an extension of earlier investigations into the effect of the electrode geometry in lead phthalocyanine gas sensors [2], and semiconducting oxide gas sensors [3,4]. Models of both the transient and steady-state responses are developed and compared with results obtained by exposing the sensors to different concentrations of ethanol vapour in air at different humidities (0 to 12,000 ppm). The results are compared with the analytical expressions developed by Gardner et al. [5] for six limiting cases. From the data we are able to determine the dominating mechanism effecting the response of the polymers, such as whether it is diffusion-rate or adsorption-rate limited. We can then determine the position of the polymers in the proposed diffusion-reaction [1] case diagram [5].

2. Device preparation

The devices investigated here comprise an alumina substrate onto which gold electrodes (250 nm thick) have been thermally evaporated using an Edwards E306A electron-beam evaporator. The gold is then patterned using conventional UV lithography and wet-etched to give a structure with eight different sizes of electrode gaps. The width of the gaps was measured using an optical microscope (Societe Geneevoise, Model MU-214B). Electrode separations were found to vary from their nominal sensor values, but typically covered the range of 11 to 55 μm. A second lithographic stage was used to open up windows in a passivating resist layer that, after a hard bake, defined the electrode areas for polymer electrodeposition. Fig. 1

* Corresponding author. Tel.: +44-1203-522595; Fax: +44-1203-418-922; E-mail: es2041@eng.warwick.ac.uk

[1] Strictly speaking the mechanism proposed for polymers is physical sorption rather than a chemical reaction.

0925-4005/99/$ - see front matter
PII: S0925-4005(99)00057-X

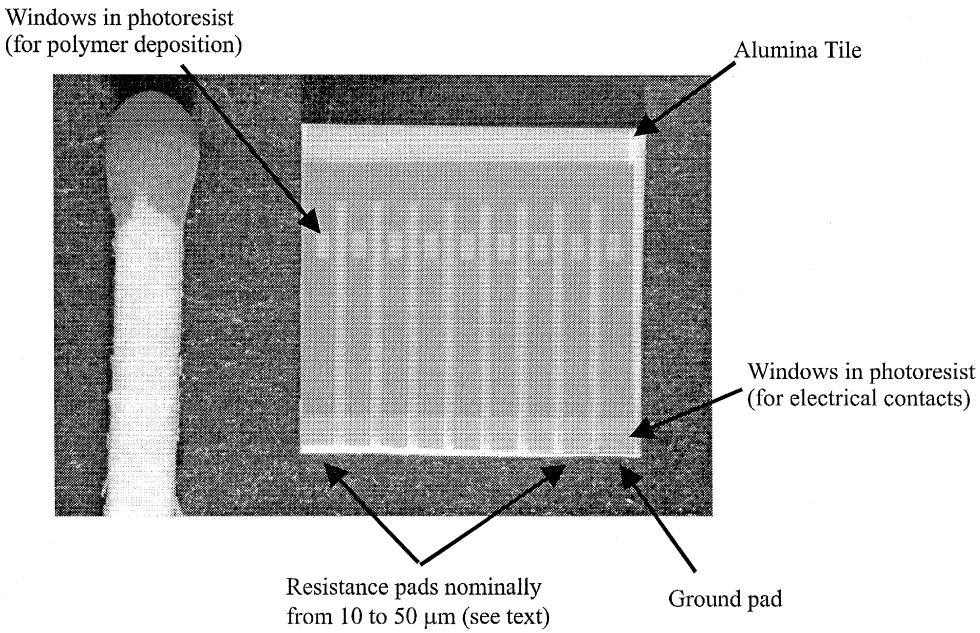

Fig. 1. Photograph of a variable gap substrate prior to deposition of the polymer membrane.

shows a variable gap device prior to the deposition of the polymer film.

The conducting polymers investigated here were grown at the University of Southampton and were poly(pyrrole) (Ppy) and poly(aniline) (Pan) systems. A standard three-electrode cell was employed, with the exposed gold regions of the micro-electrodes forming the working electrode. All of the polymer films on a particular device were deposited at the same time so as to minimise variations in the properties of the films across the different gap sizes. During the electrochemical deposition, first oxidation forms a radical cation; then a dimer is formed, either through a reaction with a second radical or by a reaction with a neutral monomer followed by oxidation. Next the dimer undergoes further oxidation and coupling reactions to build up progressively longer chains constituting the polymer film [6]. The positive charge on the resulting oxidised polymer film is balanced by the incorporation of anions from the solution as the polymer grows and by the final potential. The counter-ions employed here were chosen to represent one short- and one long-chain molecule and were pentane sulfonic acid (PSA) and decane sulfonic acid (DSA). Full details of the electrochemical deposition and characterisation of these polymer films may be found in Ref. [7].

3. Device conductance model

The polymer devices were exposed to ethanol vapour in air using a computer-controlled automated flow injection system developed at Warwick University originally for testing of lager beers [8] and subsequently modified for volatile organic vapours. Ethanol was chosen as a test vapour because this group of sensors has previously shown large and repeatable responses to polar organic compounds [9–11]. A model has been developed elsewhere in which it is assumed that a species, A, diffuses into a homogeneous thin film of thickness, L, and undergoes a Langmuir adsorption [12]. In other words, we assume that the film contains a uniform distribution, N, of immobile sites, S, with which the species can reversibly react, the reaction being described by the Langmuir adsorption isotherm, that is

$$A + \langle S \rangle \underset{k_h}{\overset{k_f}{\Leftrightarrow}} \langle A \rangle \tag{1}$$

where k_f and k_b are the forward and backward reaction rate constants, respectively. Exploiting the geometry of a planer film allows the use of a one dimensional model in which the sorbate concentration, a, and site occupancy, θ, profiles are only a function of the distance x and time t.

The process can then be described by a modified diffusion equation in dimensionless form,

$$\frac{\partial^2 \gamma}{\partial \chi^2} - \frac{\partial \gamma}{\partial \tau} = \frac{\eta}{\lambda} \frac{\partial \theta}{\partial \tau} \tag{2}$$

where χ is the dimensionless distance parameter (x/L), L is the depth of the polymer, τ is the dimensionless time parameter (Dt/L^2), γ the normalised gas concentration

(a/a_∞) and a_∞ is the external gas concentration. η and λ are dimensionless parameters given by KN and Ka_∞, respectively, and therefore depend on the material properties such as the binding constant K (k_f/k_b) and the density of sites N [5], see Fig. 2.

The vapour that is bound (or released on desorption) from the diffusion process by sites can be related to the sorption kinetics by,

$$\eta\frac{\partial\theta}{\partial\tau} = \kappa\lambda\gamma(1-\theta) - \kappa\theta \tag{3}$$

where κ is a dimensionless parameter that equals the ratio of the adsorption rate to the diffusion rate. Eqs. (2) and (3) can be solved with suitable boundary conditions to obtain the site occupancy $\theta(\chi,\tau)$ profiles. Fig. 3 shows the case diagram that contains the full solution space defined by κ, λ and η with the six limiting Cases I to VI marked on it. Case I ($\lambda<1,\ \eta<1,\ \kappa<\eta$) describes a pure diffusion process where the diffusion rate is far slower than the adsorption rate and there are few adsorption sites to modify the diffusion process. Case II ($\lambda<1,\ \eta>1,\ \kappa<1$) is again a diffusion-limited case. However, in this case there is a significant number of sites that slow down the diffusion process (by a factor of $\sim 1/\eta$). In case III ($\lambda<1,\ \kappa<1,\ \kappa<\eta$) the adsorption rate is far slower than the diffusion rate and therefore the process is adsorption rate limited. The reaction kinetics are in the linear (unsaturated) region of the isotherm, i.e., most of the sites within the polymer are unoccupied. Case IV ($\lambda>1,\ \kappa<1,\ \kappa<\eta$) is also an adsorption-rate limited process. However, this case describes the saturated region of the isotherm, i.e., most of the sites within the polymer are occupied. Case V ($\lambda>1,\ \lambda^2>\eta,\ \kappa<1,\ \kappa>\eta$) describes the saturated region of the isotherm where the kinetics are fast so that equilibrium is maintained between free and bound species. Finally, in case VI ($\lambda>1,\ \lambda^2<\eta,\ \eta>1,\ \kappa<1$) neither diffusion nor adsorption dominates the process and a moving boundary problem is encountered.

The transient and steady-state conductance of polymeric devices can therefore be fully described by combining the site occupancy profiles with the electric field distribution within the polymer. For a pair of semi-infinite thin electrodes with a separation of w and a length b (i.e., $b \gg w$) the electric field, E, has been determined using Schwartz–Christoffel transformations [4] to be,

$$E(\chi,0) = \frac{V}{L\pi}\Big/\sqrt{\chi^2 + w^2/4L^2} \tag{4}$$

where V is the voltage applied across the electrodes. This equation assumes that there is a constant medium in the semi-infinite region above the electrodes. However, any difference in the dielectric permittivities of the polymer, substrate or air/vapour will have an effect on the distribution of the *displacement* lines. We believe the device's response is not sensitive to this phenomenon because the device conductance is calculated by integrating the *electric* field along a line through the structure. The parametric form of Eq. (4) has also been verified experimentally by data reported by Bartlett et al. [13].

In our model we assume that the conductivity of the polymeric film is given by,

$$\sigma(\chi,\tau) \approx \sigma_{00}[1 - S_h\theta_h - S_e\theta_e] \tag{5}$$

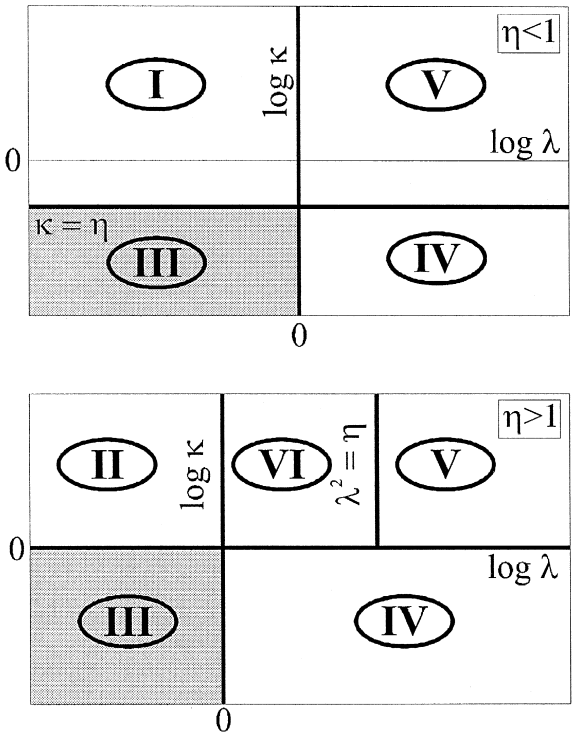

Fig. 3. Case diagram showing solutions to the diffusion reaction problem: I—pure diffusion; II—slow diffusion; III—unsaturated (linear) reaction kinetics; IV—saturated reaction kinetics; V—saturated (nonlinear) reaction kinetics; VI—mixed diffusion reaction process.

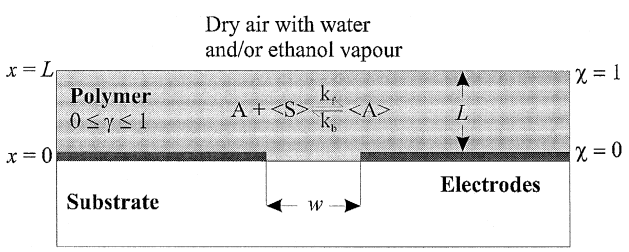

Fig. 2. Schematic diagram of a polymer chemoresistor with model parameters defined.

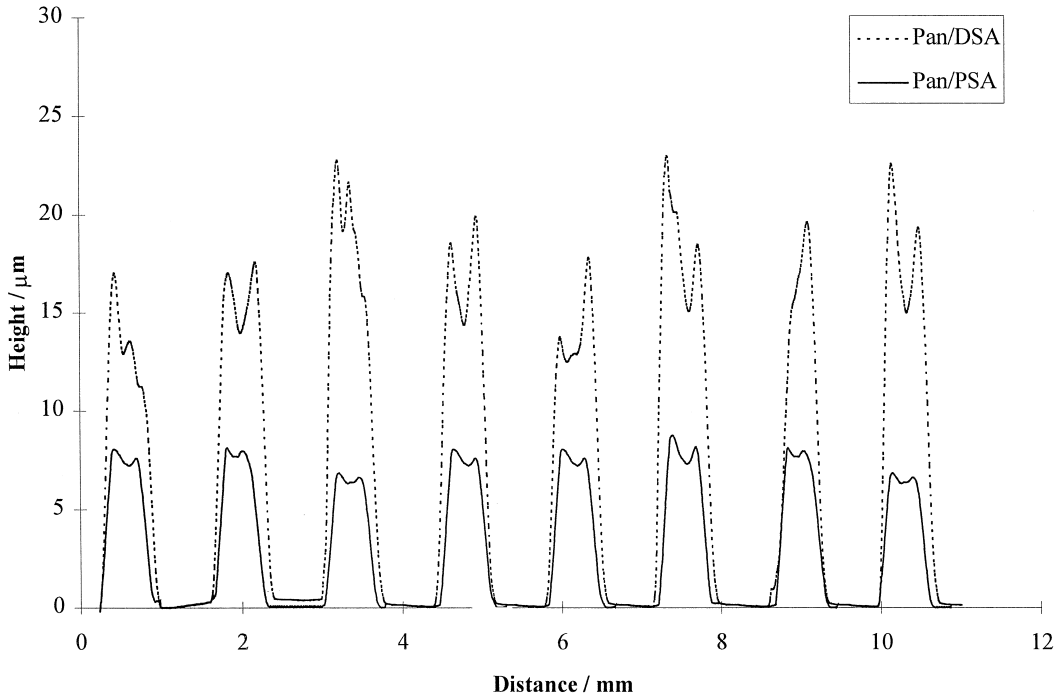

Fig. 4. A talysurf profile of Pan/DSA/H_2O and Pan/PSA/H_2O sensors.

where S_e and S_h are sensitivity coefficients to ethanol and water, respectively, and σ_{00} is the conductance of the device when neither water nor ethanol vapour are present.

The current passing through a device can therefore be calculated by integrating the product of the local conductivity and the electric field over a closed surface. We can then define the fractional response of a device as, [2]

$$\frac{G(\tau)-G_0}{G_0}=\frac{1}{1-S_h\theta_h}\times\left[S_h\Delta\theta_h-S_e\frac{\int_0^1\theta_e(\chi,\tau)/\sqrt{\chi^2+w^2/4L^2}\,d\chi}{\ln\left[\frac{1+\sqrt{(1+w^2/4L^2)}}{w/2L}\right]}\right] \quad (6)$$

Where G_0 is the steady-state baseline conductance of the device at a constant absolute humidity and $\delta\theta_h$ is the change in the proportion of sites occupied by water when the ethanol vapour is introduced.

This model assumes that the water and ethanol vapours are absorbed by the same sites, i.e., a *competitive* binding model. The proportion of sites occupied by water when no ethanol vapour is present, θ'_h, can then be given by,

$$\theta'_h=\frac{K_h a_h}{(1+K_h a_h)} \quad (7)$$

and when ethanol is present the proportion occupied by water and ethanol are given by,

$$\theta''_h=\frac{K_h a_h}{(1+K_h a_h+K_c a_c)} \quad \theta_e=\frac{K_e a_e}{(1+K_c a_e+K_h a_h)} \quad (8)$$

The steady-state response (in terms of device conductance) can now be defined in terms of the fractional site occupancy by

$$\frac{G(\tau\to\infty)-G_0}{G_0}\approx\frac{S_h(\theta'_h-\theta''_h)-S_e\theta_e}{(1-S_h\theta'_h)} \quad (9)$$

The size of the steady-state response for homogeneous conducting polymer films with a uniform distribution of absorbent and sites therefore depends on the magnitude of the sensitivity terms but not on the device geometry.

4. Results

4.1. Surface profiles

Any modelling of the properties of the polymers first requires knowledge of the thickness of the polymer mem-

[2] This assumes that the displaced water molecules do not contribute to the bulk conductance.

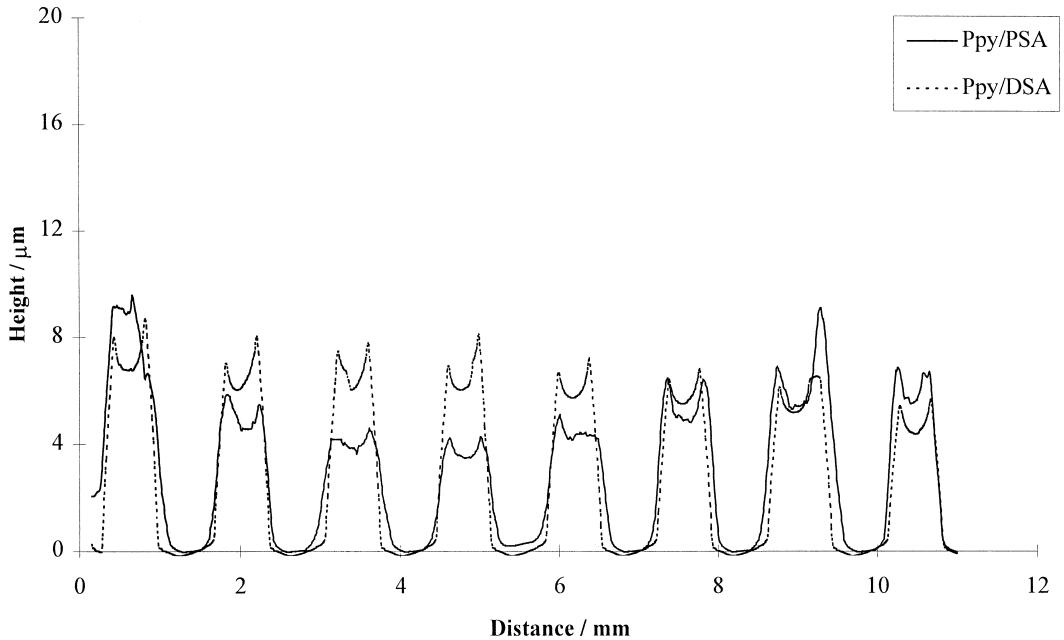

Fig. 5. A talysurf profile of Ppy/DSA/H_2O and Ppy/PSA/H_2O sensors.

brane. In order to achieve this surface profiles of the devices employed during testing were carried out using a Taylor–Hobson form talysurf. The profiles for poly(aniline) and poly(pyrrole) sensors are shown in Figs. 4 and 5, respectively. These results show that the thickness of the film does not vary significantly over the range of gap sizes used for each polymer. The dip seen in the middle of the films could be caused by either differential drying or preferential polymer growth near the electrode edges because of easier mass transport.

It is interesting to note that although the electrode separation does not seem to significantly modify the thickness of the films, the different types of polymer have been grown to different thickness. This can be attributed to the different growth solutions used and to differences in the deposition kinetics for the different polymers.

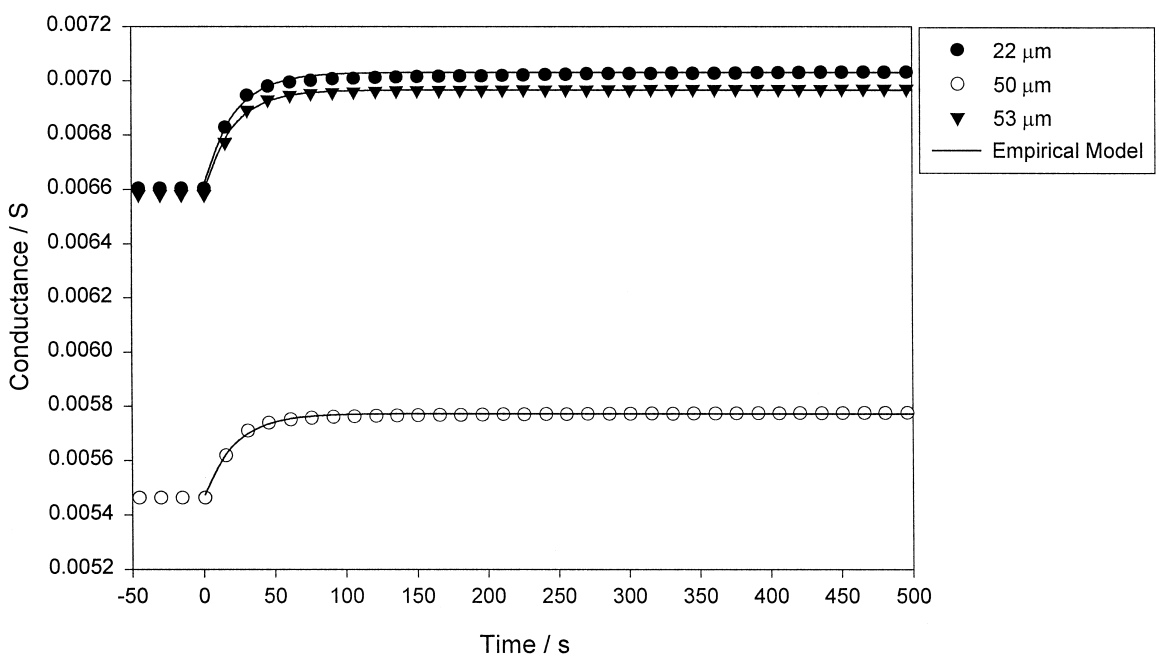

Fig. 6. A diagram showing the on transient for Pan/DSA/H_2O when exposed to a concentration of 26,336 ppm ethanol at a constant humidity of 2328 ppm and temperature of 35.3°C. Three electrode separations 22, 50 and 53 μm are shown.

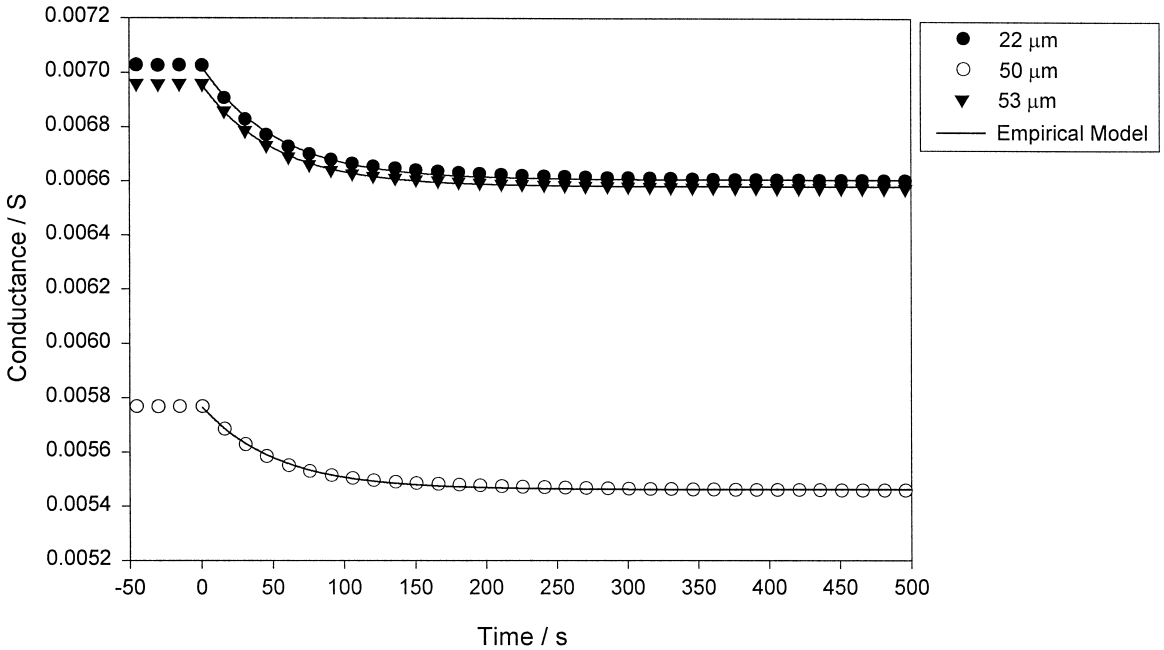

Fig. 7. A diagram showing the off transient for Pan/DSA/H_2O when exposed to a concentration of 26,336 ppm ethanol at a constant humidity of 2328 ppm and temperature of 35.3°C. Three electrode separations 22, 50 and 53 μm are shown.

4.2. Transient responses

In order to explore the effects of gap size, analyte concentration etc. on the transient responses of conducting polymer sensors, we first need to develop an empirical expression that can successfully model the on and off transients of the sensors. The expressions employed to describe the poly(aniline) on and off transients are given in Eqs. (10) and (11) respectively,

$$(G(t) - G_0) = \Delta G\left[1 - \exp\left(-\frac{t}{t_{on}}\right)\right] \quad (10)$$

$$(G(t) - G_0) = \Delta G\left[\exp\left(-\frac{t}{t_{off}}\right)\right] \quad (11)$$

where $G(t)$ is the conductance of the polymer at time t, G_0 is the baseline conductance of the polymer, i.e., in the absence of ethanol vapour, ΔG is the change in conductance of the sensor due to the ethanol concentration and t_{on} and t_{off} are the time constants for the on and off responses, respectively. Figs. 6 and 7 show examples of the on and off transients for Pan/DSA/H_2O. The empirical model is also shown on these diagrams. This demonstrates an excellent fit to the experimental data with the correlation coefficient for both the on and off transients greater than 0.99.

The empirical expressions employed to model the transients for the Pan sensors did not give satisfactory correlation for Ppy. For this group of polymers a double-exponential expression was used to model the generally longer time responses and the drift demonstrated during exposure. Eqs. (12) and (13) were used for the on and off transients respectively, [3]

$$G(t) - G_0 = \Delta G_1\left[1 - \exp\left(-\frac{t}{t_{on1}}\right)\right] + \Delta G_2\left[1 - \exp\left(-\frac{t}{t_{on2}}\right)\right] \quad (12)$$

$$G(t) - G_0 = \Delta G_1\left[\exp\left(-\frac{t}{t_{off1}}\right)\right] + \Delta G_2\left[\exp\left(-\frac{t}{t_{off2}}\right)\right] \quad (13)$$

These expressions divide the response of the Ppy sensors into two components: the first is an initial response due to the exposure of the ethanol vapour; and the second component is a long-term response either due to the ethanol vapour or due to drift within the polymer. The value of the time constants for the second component of both the on and off transients (t_{on2} and t_{off2}) were very large, generally greater than 3000 s, and also seemed to be independent of the ethanol concentration. This seems to suggest that the second component of the expression is due to drift in the polymers and therefore should not be included in the analysis of the ethanol response. Figs. 8 and 9 show examples of the on and off transients for three gaps coated

[3] Note that ΔG takes a negative sign here for poly(aniline) films.

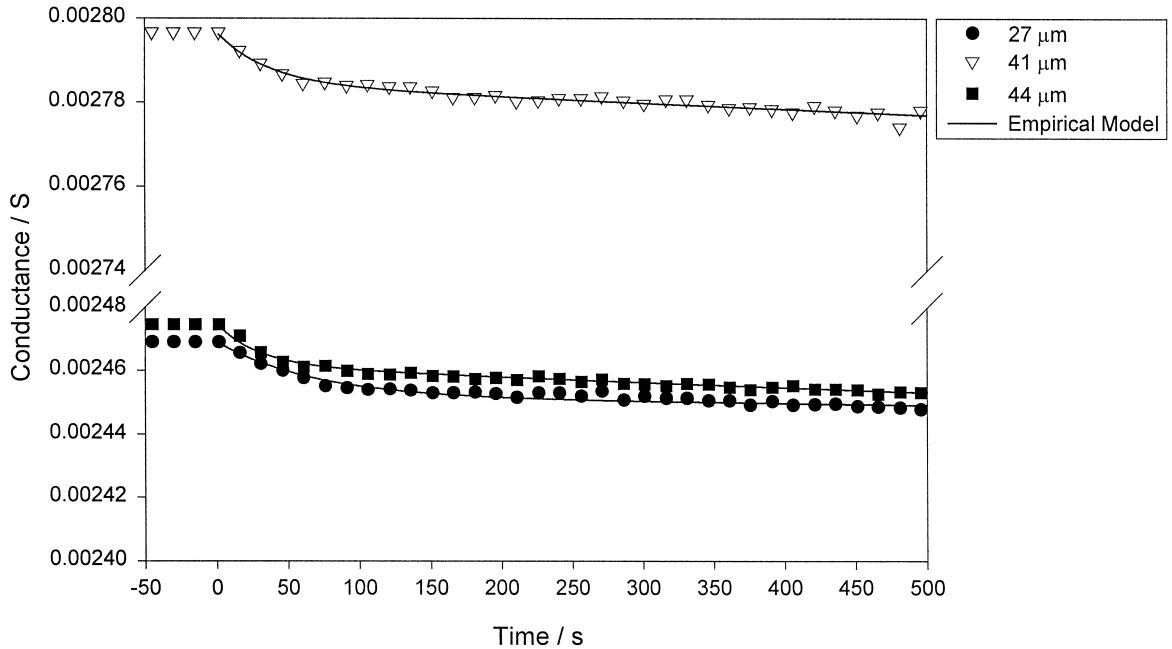

Fig. 8. A diagram showing the on transient for Ppy/PSA/H_2O when exposed to a concentration of 26,336 ppm ethanol at a constant humidity of 2328 ppm and temperature of 35.8°C. Three electrode separations 27, 41 and 44 μm are shown.

with Ppy/PSA/H_2O. The empirical model of the responses is also shown. Although the correlation between this model and the data is not as good as that demonstrated for the Pan sensors, a reasonable fit was still obtained with the correlation coefficient generally greater than 0.71.

Assuming that the transients are not limited by mixing in the mass flow system, the symmetry of the on and off transients shown in Figs. 6–9 can now be employed to determine some of the physical properties of these polymers. In Cases IV and V the boundary conditions assume

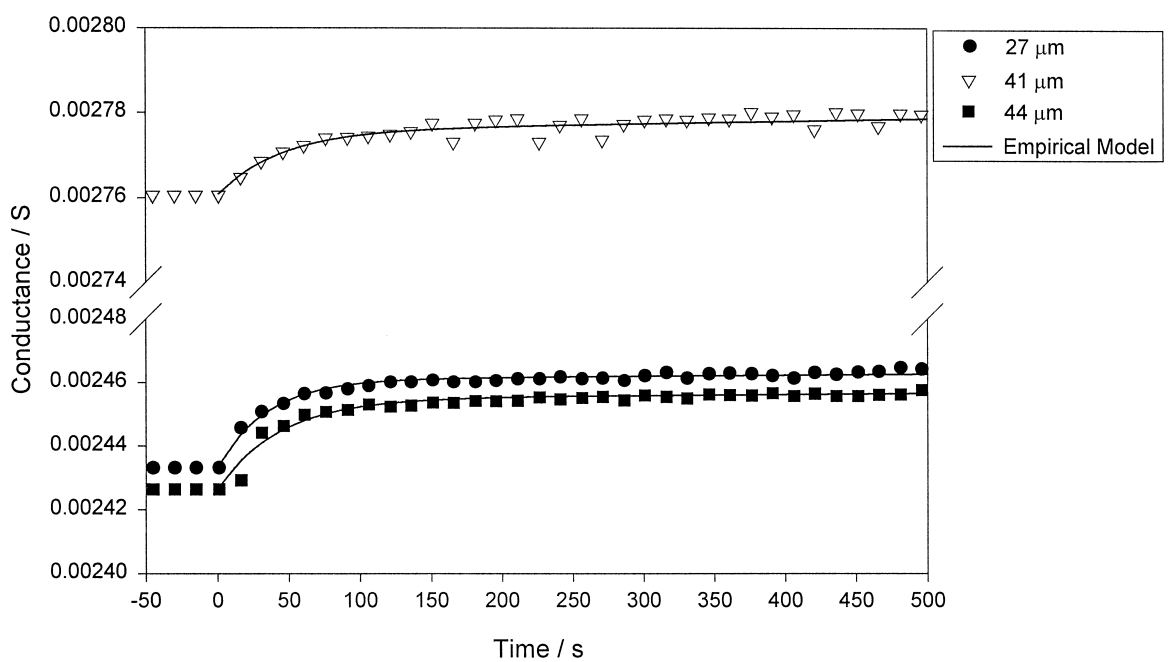

Fig. 9. A diagram showing the off transient for Ppy/PSA/H_2O when exposed to a concentration of 26,336 ppm ethanol at a constant humidity of 2328 ppm and temperature of 35.8°C. Three electrode separations 27, 41 and 44 μm are shown.

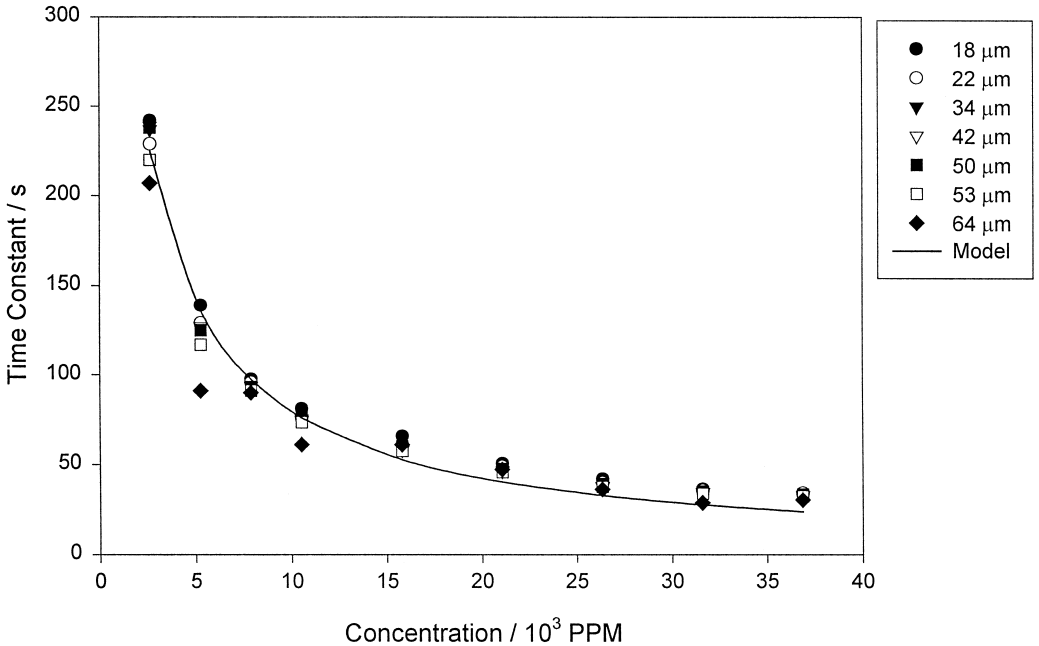

Fig. 10. A graph showing the effect of ethanol concentration on the time constant of Pan/DSA/H_2O at constant humidity (2328 ppm) and temperature (35.3°C). A range of electrode separations is shown.

that the polymers are adsorption-rate limited and that saturation is reached ($\theta \approx 1$). This means that there is a larger concentration of the target vapour and only a few sites with which it can react. Therefore the sites fill quickly but upon desorption a large amount of the vapour has to leave before the sites are emptied. This means that the off transient for the exposure should take far longer than the on (i.e., the on and off transients are asymmetric). Case VI also assumes that the sites become saturated. Although in this case neither the reaction or diffusion kinetics dominate the response we should still observe differences between the on and off transients. Figs. 6–9 show that the transients observed for both Pan and Ppy are almost perfectly symmetric with typical on and off time constants varying by less than 2%. We can therefore deduce that, at equilibrium most of the sites in the poly-

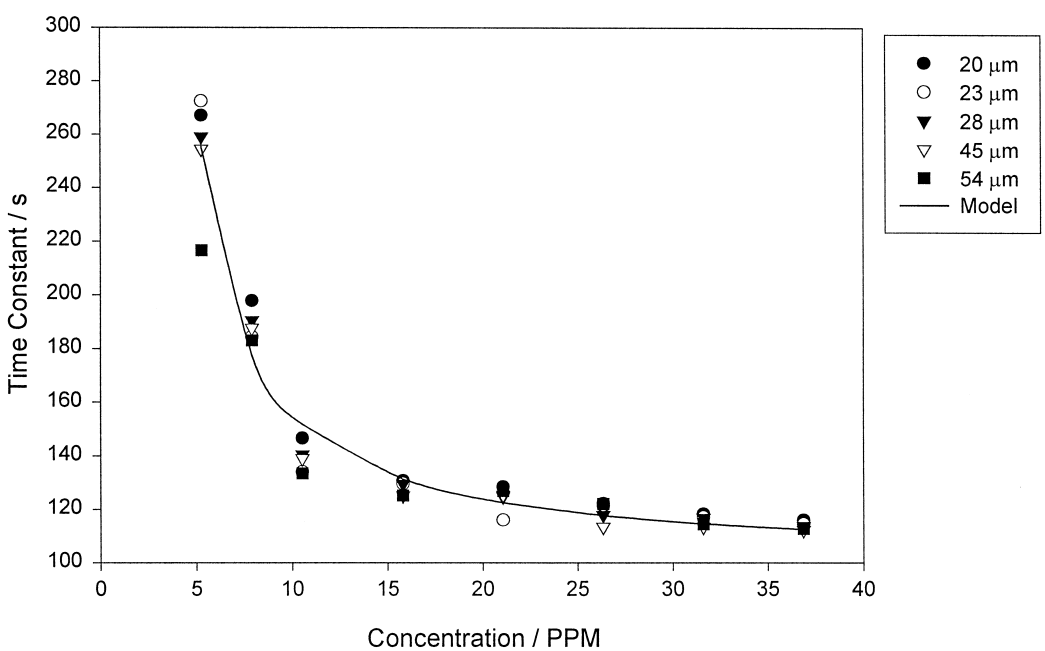

Fig. 11. A graph showing the effect of ethanol concentration on the time constant of Ppy/DSA/H_2O at constant humidity (2328 ppm) and temperature (35.8°C). A range of electrode separations is shown.

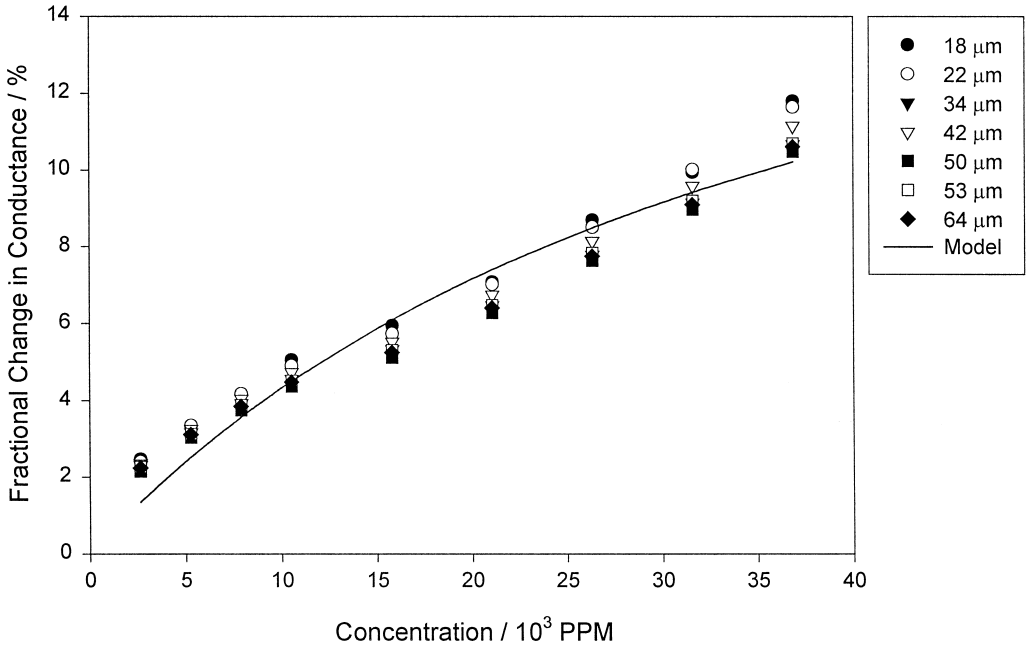

Fig. 12. A graph showing the effect of ethanol concentration on the magnitude of the fractional response of a Pan/DSA/H_2O sensor at constant humidity (1164 ppm) and temperature (35.3°C). A range of electrode separations is shown.

mers tested are unoccupied ($\lambda < 1$) and we can conclude that we are not working in Cases IV, V or VI.

In order to distinguish between the remaining cases we need to determine whether the polymers are limited by their diffusion or adsorption rate. If the reaction of the vapour with the available sites was almost instantaneous when compared with its diffusion through the film (diffusion-rate limited), we would expect to see a large dependence of the time constant on the electrode separation at constant film thickness. This is due to the electric field distribution within the membrane altering as the electrode separation changes, i.e., the inner part of the films has a more significant effect on the conductance for the narrow electrode spacing than for the wider spacing. Both the

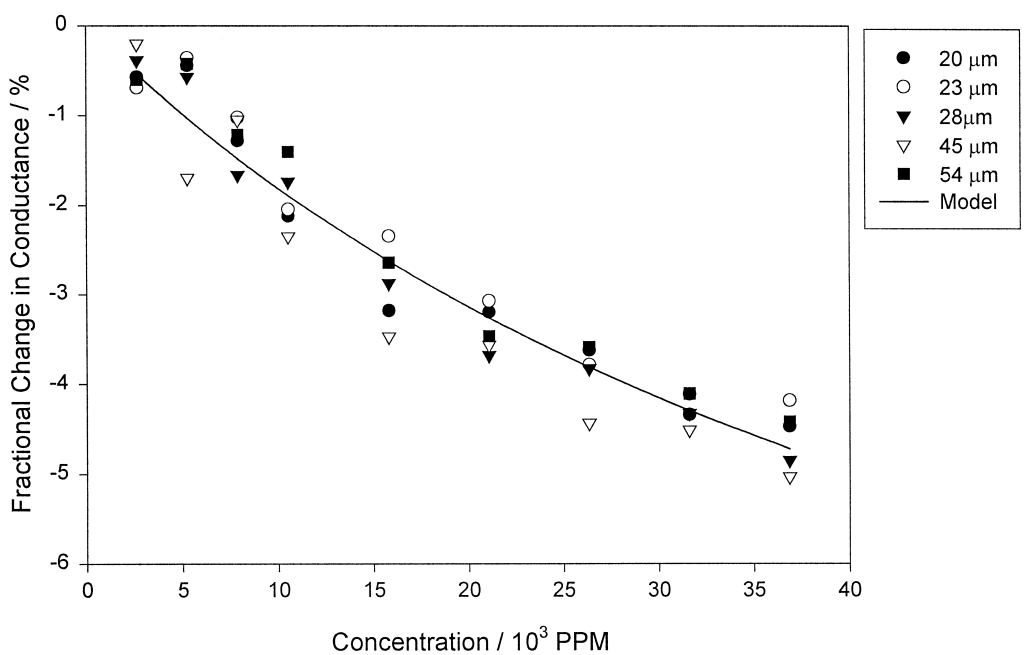

Fig. 13. A graph showing the effect of ethanol concentration on the magnitude of the fractional response of a Ppy/DSA/H_2O sensor at constant humidity (1164 ppm) and temperature (35.8°C). A range of electrode separations is shown.

diffusion-rate limited cases also include the postulate that the diffusion coefficient is independent of the vapour concentration. Therefore, we would expect the time constant to be independent of the analyte concentration. In Case III (adsorption-rate limited) we would expect to see a large dependence of the time constant on the vapour concentration as the Langmuir sorption kinetics, defined by Eq. (1), would be dominating the response. However, for this type of case we would not expect to observe a dependence of the time constant on the electrode separation. Figs. 10 and 11 show the time constant for different gap sizes against ethanol concentration for a Ppy and Pan sensor. These results show that, within experimental error, the electrode geometry has little or no effect on the time constant of the polymers, and that the vapour concentration has a large influence. We can therefore conclude that the polymers are adsorption-rate limited in the linear portion of the isotherm (Case III).

4.3. Steady-state responses

We can now investigate the steady-state responses of the polymers (time $t \gg t_{on}$). Eq. (9) predicts that the response of the polymers will be independent of the electrode separation at a constant humidity and temperature. This effect is demonstrated within experimental error and examples for Ppy and Pan can be seen in Figs. 12 and 13.

Finally, the model postulated in Eq. (6) assumed that the water and ethanol vapours are adsorbed by the same sites, i.e., a competitive binding model. Eqs. (7) and (8) defining the proportion of sites occupied in the absence and in the presence of ethanol vapour respectively can now be combined with Eq. (9), giving,

$$\frac{G(t \gg t_{on}) - G_0}{G_0} \approx \frac{\dfrac{(-S_h K_h a_h - S_e K_e a_e)}{(1 + K_h a_h + K_e a_e)} + \dfrac{S_h K_h a_h}{(1 + K_h a_h)}}{\left[1 - \dfrac{S_h K_h a_h}{(1 + K_h a_h)}\right]} \quad (14)$$

This model has been employed for a single gap (10 μm) at a constant temperature. The concentration of both ethanol and water vapours have been systematically varied and the responses observed. Due to the competitive nature of the model, as the water concentration is increased the response to the ethanol vapour reduces. This effect can be clearly seen for examples of Ppy and Pan sensors in Figs. 14 and 15.

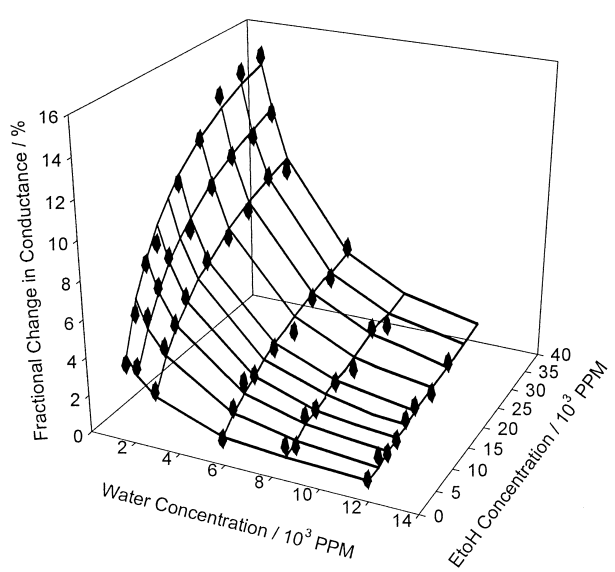

Fig. 14. Typical plot of the effect of water and ethanol vapour on the response of Pan/DSA/H_2O gas sensors at 23.7°C. The solid mesh is a fit of the theory to the experimental data.

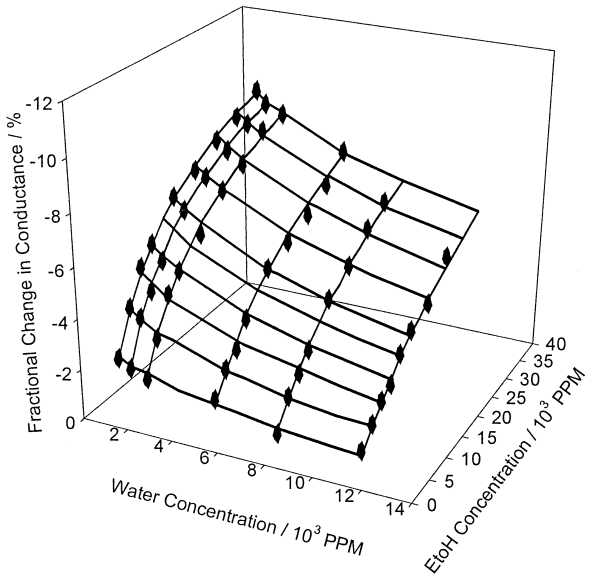

Fig. 15. Typical plot of the effect of water and ethanol vapour on the response of Ppy/DSA/H_2O gas sensors at 23.7°C. The solid mesh is a fit of the theory to the experimental data.

5. Conclusions

We have developed a theory to explain the effect of electrode geometry upon the response of thin-film conducting polymer resistive gas sensors. The theory describes the transient response as *adsorption-rate* limited (known by us as Case III) and steady-state response in wet air by a new competitive binding model. The theory has been tested against experimental data on ethanol vapour and the results show good agreement.

Acknowledgements

The authors wish to thank Ms. S. Friel (Warwick University) for the design of the multi-electrode structure, and Dr. J. Elliott (Southampton University) for the deposition of the conducting polymer films.

References

[1] J.J. Miasik, A. Hooper, B.C. Tofield, Conducting polymer gas sensors, J. Chem. Soc., Faraday Trans. 82 (1986) 1117–1126.
[2] J.W. Gardner, M.Z. Iskandarani, B. Bott, Effect of electrode geometry on gas sensitivity of lead phthalocyanine thin films, Sensors and Actuators B 9 (1992) 133–142.
[3] U. Jain, A.H. Harker, A.M. Stoneham, D.E. Williams, Effect of electrode geometry on sensor response, Sensors and Actuators B 2 (1990) 111–114.
[4] J.W. Gardner, Electrical conduction in solid-state gas sensors, Sensors and Actuators 18 (1989) 373–387.
[5] J.W. Gardner, P.N. Bartlett, K. Pratt, Modelling of gas-sensitive conducting polymer devices, IEE Proc.: Circuits, Devices and Systems 142 (1995) 321–333.
[6] G.K. Chandler, D. Pletcher, The electrochemistry of conducting polymers, Specialist Periodical Reports, Electrochemistry, 10, Royal Society of Chemistry, London, 1985.
[7] J. Elliot, PhD thesis, University of Southampton, UK, 1997.
[8] J.W. Gardner, T.C. Pearce, S. Friel, P.N. Bartlett, N. Blair, Multisensor system for beer flavour monitoring using an array of conducting polymers and predictive classifiers, Sensors and Actuators B 18 (1994) 240–243.
[9] P.N. Bartlett, S.K. Ling-Chung, Conducting polymer gas sensors: Part 3. Results for 4 different polymers and 5 different vapours, Sensors and Actuators 20 (1989) 287–292.
[10] P. Ingleby, J.W. Gardner, P.N. Bartlett, A competitive binding model for the response of poly(pyrrole) and poly(aniline) chemoresistors, in preparation.
[11] P. Topart, M. Josowicz, Characterisation of the interaction between poly(pyrrole) films and methanol vapour, J. Phys. Chem. 96 (1992) 7824–7830.
[12] P.N. Bartlett, J.W. Gardner, Diffusion and binding of molecules to sites within homogeneous thin films, Trans. R. Soc. London A 354 (1996) 35–57.
[13] P.N. Bartlett, P. Archer, S.K. Ling-Chung, Conducting polymer gas sensors: Part 1. Fabrication and characterisation, Sensors and Actuators 19 (1989) 125–140.